

# Dynamical Heterogeneities in Grains and Foams

Olivier Dauchot

*SPEC, CEA-Saclay, 91 191 Gif-sur-Yvette, France*

Douglas J. Durian

*University of Pennsylvania, Department of Physics and Astronomy, Philadelphia, PA  
19104-6396, USA*

Martin van Hecke

*Kamerlingh Onnes Laboratory, Universiteit Leiden, Postbus 9504, 2300 RA Leiden, The  
Netherlands*

**OXFORD**  
UNIVERSITY PRESS



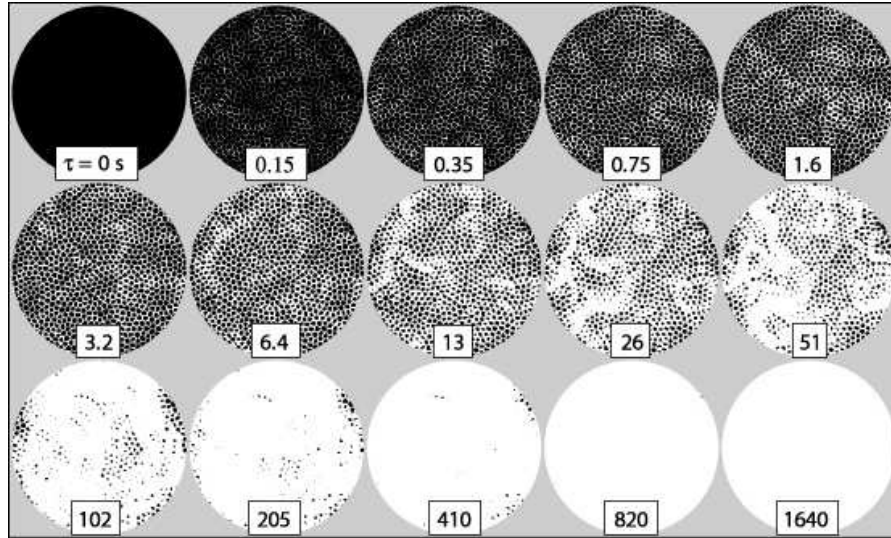


**Fig. 0.1** An illustration of dynamical heterogeneities in an air-fluidized monolayer of beads at an area packing fraction of 0.79 (from Ref. (Abate and Durian, 2007)). The Voronoi tessellation is computed at each time step and the white regions represent for each bead the space that has come outside of the initial Voronoi cell after a delay  $\tau$  as labelled in the figure.

## Abstract

Dynamical heterogeneities have been introduced in the context of the glass transition of molecular liquids and the lengthscale associated with them has been argued to be at the origin of the observed quasi-universal behaviour of glassy systems. Dense amorphous packings of granular media and foams also exhibit slow dynamics, intermittency and heterogeneities. We review a number of recent experimental studies of these systems, where one has direct access to the relevant space-time dynamics, allowing for direct visualisations of the dynamical heterogeneities. On one hand these visualisations provide a unique opportunity to access the microscopic mechanisms responsible for the growth of dynamical correlations. On the other hand focussing on the differences in these heterogeneities in microscopically different systems allows to discuss the range of the analogies between molecular thermal glasses and athermal glasses such as granular media and foams. Finally this review is the opportunity to discuss various approaches to actually extract quantitatively the dynamical lengthscale from experimental data.

## 0.1 Introduction

Granular media and foams exhibit a wide range of complex flow phenomena, some familiar, some surprising, but often poorly understood (Jaeger *et al.*, 1996; Cates *et al.*, 1998; Liu and Nagel, 2001; Duran, 2000; MiDi, 2004; Aranson and Tsimring, 2006; Kraynik, 1988; Wilson, 1989; Prud’homme and Khan, 1996; Weaire and Hutzler, 1999; Dauchot, 2007).

The constituents of these materials, macroscopic grains and gas bubbles, are so large that thermal fluctuations do not cause appreciable agitations, and their interactions are dissipative. Hence, when unperturbed, these material jam into a metastable, disordered state, and to create dynamics energy needs to be supplied, in the form of, e.g., shearing or vibrations.

The reason why these materials feature in a book on glasses is that their dynamical behavior often is “glassy” — slow dynamics, intermittency and heterogeneities are key phrases in describing their behavior. For example, when repeatedly tapping a loose packing of grains, their density slowly increases, but instead of exhibiting an exponential relaxation to an asymptotic density, the relaxation process is logarithmically slow and, moreover, exhibits memory effects, evidencing aging (see (Dauchot, 2007) for a review). In addition, when granular media flow, they typically do so inhomogeneously. Far away from the main flowing region this results in very slow creeping flows, where fluctuations are relatively large and where the response is sluggish. Foams exhibit similar phenomenology.

Dynamical heterogeneities are a key characteristic of glassy dynamics in thermal systems (Sillescu, 1999; Ediger, 2000; Glotzer, 2000; Lacevic *et al.*, 2003; Cipelletti and Ramos, 2005), so a natural question to ask is the nature and organization of the fluctuations in granular media and foams. As we will outline in this chapter, the macroscopic glassy features of these materials are indeed accompanied by heterogeneous fluctuations at the microscopic, i.e., bubble or grain scale. To wet the readers appetite, in Fig. 0.1 we show a graphic example of dynamical heterogeneity in topviews of a system of air fluidized beads. The coloring in this graph represents the persistent area order parameter, which quantifies how much the area of the voronoi cell surrounding a grain has changed in a given lag time. Note that the dynamics appear homogeneous at early and long times, but are spatially heterogeneous at intermediate times - most noticeably for the images at  $13 \text{ s} \leq \tau \leq 102 \text{ s}$ .

We will focus here on examples of heterogeneous dynamics of foams and granulates. Since crowding plays a crucial role for these materials in their dense, glassy phase, one should perhaps not be surprised that grain and bubble motion is inherently heterogeneous, and that fluctuations become spatially correlated — for one grain to move in a dense system, many other grains have to get out of the way. Open questions include how far one can push the analogies between molecular and colloidal glasses on the one hand, and foams and granular media on the other hand, and what one can learn about the differences in the heterogeneities in microscopically different systems.

An important experimental advantage of granular media and foams is that one has direct access to the relevant space-time dynamics, allowing for direct observations of the heterogeneous behavior. Moreover, these materials can be brought close to and often through a jamming transition, in the vicinity of which dynamical properties can be expected to change dramatically with control parameters. Finally, grains and

foams have different microscopic interactions, that are quite well understood — grains are essentially undeformable and have inelastic and frictional interactions, whereas foam bubbles are easily deformed and have viscous interactions. Hence, by comparing their behavior, robustness of various glass forming / jamming / heterogeneity scenarios can be probed. Moreover, the more complex interactions of grains makes that heterogeneities can be probed in two physically distinct regimes — a relatively low packing density regime where grain interactions are dominated by collisions, and a higher density regime where frictional contacts dominate the interactions.

The term “jamming” has evolved to have many meanings. It was originally proposed as an umbrella concept, meant to apply equally to the glass transition in molecular and colloidal liquids as to the cessation of flow in grains and foams (Liu and Nagel, 2001). Two different definitions are offered in Ref. (O’Hern *et al.*, 2003*b*). The first is that jamming is said to occur when a system develops a yield stress, and hence has mechanical rigidity. However as a practical matter it is not possible to test whether a material truly has a yield stress, or whether the stress relaxation time is too long to measure. So alternatively jamming is said to occur when a system develops a relaxation time that exceeds a reasonable experimental timescale, eg. 1000 s. This is similar in spirit to defining the glass transition to occur when the viscosity exceeds  $10^{13}$  poise, a large but arbitrary value. These two definitions are perfectly consistent when the relaxation time refers to rigidity, in terms of the decay time of the macroscopic shear stress relaxation modulus. However it’s a different notion, not always well distinguished in the literature, to define jamming in terms of the timescale for microscopic reorganization of structural degrees of freedom like the set of topological nearest neighbors. Here, we often use jamming in a rather loose sense, referring to dramatic slowing down of the dynamics and a qualitative change of the behavior from freely flowing to being stuck.

The outline of this chapter is as follows. In section 0.2 we discuss heterogeneities in agitated granular media. These include air fluidized granular system where the grain interactions are dominated by collisions, the grains are driven randomly and isotropically, and the system is quasi-two dimensional (section 0.2.1), and dense 2D granular systems where grain interactions are frictional (sections 0.2.2 and 0.2.3). In section 0.2.2 the system is driven by slow oscillatory shear, and real space rearrangements play a role, while in section 0.2.3 the system is driven by horizontally shaking its support plate, and real space rearrangements are substantially less than one grain diameter during the duration of the experiment. In section 0.3 we describe observations of heterogeneities in granular flows in inclined plane, rotating drum and pile-flow geometries — for these flows, the grain interactions are a mix between collisions and enduring contacts, the flow is driven by bulk shear forces, and the system is three dimensional. Finally, in section 0.4 we describe observations of heterogeneities and large fluctuations in foams. We close this chapter by a discussion of commonalities and differences between these systems, and in the appendix discuss various approaches for calculating the dynamical susceptibility  $\chi_4$  which quantifies the dynamical heterogeneities. The reader who is not familiar with dynamical susceptibilities and how they relate to four point dynamical correlators should refer to this appendix and the first chapters of the present book.

## 0.2 Heterogeneities in Agitated Granular Media

### 0.2.1 Growing dynamical lengthscale in a monolayer fluidized bed

Quasi-two dimensional monolayers of shaken, sheared, and fluidized grains have been important as model systems, both because it's difficult to adequately probe an opaque 3d medium but more crucially because their packing density may be controlled and varied free from gravitational compaction. For fluidization, the setup involves a sub-monolayer of beads that typically roll without slipping upon a fine screen up through which air is uniformly blown. The upward drag need not fully offset gravity to excite motion - rather, the grains are stochastically kicked within the plane by the shedding of turbulent vortices. As reported in Ref. (Abate and Durian, 2006) the air-fluidized grains therefore experience random ballistic motion at short times and random diffusive motion at long times. At intermediate times, and at high enough densities, the grains also exhibit an interval of subdiffusive motion where they collide multiple times with a long-lived set of neighbors. As the packing density is increased, the duration of this “caging” increases until all motion ceases at random close packing. Concurrently, there is little change in packing structure, though the pair correlation function does exhibit a growing first peak and a split second peak.

On approach to jamming by addition of grains to increase the packing density, the dynamics slows down and becomes heterogeneous as illustrated on figure 0.1. This has been quantified by measures of the cluster size and of the chain length for the intermittent fast-moving regions, as well as through use of dynamic four-point susceptibilities based on three similar order parameters, which essentially characterize how much the local structure has evolved (see appendix). Data for the one based on the overlap of the Voronoi tessellation (see fig. 0.1) are plotted in Fig. 0.2 for a sequence of different packing fractions. The upper plot is a measure of the temporal relaxation averaged over the whole system. It clearly demonstrates the slowing down of the dynamics when the packing fraction increases. The bottom one shows that the peak in the corresponding susceptibility rises on approach to jamming indicating the presence of a growing length scale (Keys *et al.*, 2007).

### 0.2.2 Building blocks of Dynamical Heterogeneities

Recently, the dynamics of a dense bidisperse monolayer of disks under cyclic shear has been investigated in Saclay (Marty and Dauchot, 2005; Dauchot *et al.*, 2005; Candelier *et al.*, 2009a). The experimental setup is shown in Fig. 0.3-lhs). The dominant feature of the grain trajectories is the so-called cage effect (see fig. 0.3-rhs): at short times, particles are trapped by their neighbors, while at longer times particles leave their cage and diffuse through the sample by successive cage jumps. In these experiments the packing fraction is large and cage jumps necessarily lead to displacements of neighboring particles — this observation is at the root of the idea of cooperative motion and dynamical heterogeneities.

As is illustrated in figure 0.4, cage jumps are organized in clusters which avalanche to built up the long term dynamical heterogeneities (Candelier *et al.*, 2009a). The distribution in space and time of the cage jumps is far from homogeneous. The left panel of figure 0.4 illustrated that cage jumps form clusters in space, occurring on a

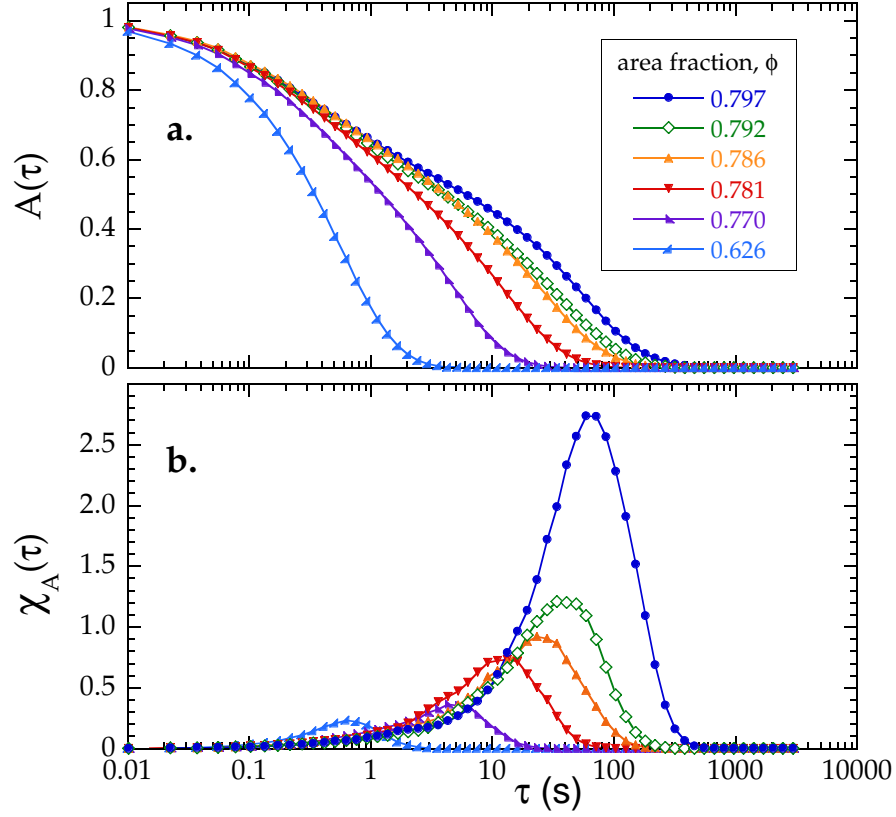


**Fig. 0.2** (a) Average relaxation, and (b) associated susceptibility, vs delay time for a sequence of packing fractions in the monolayer fluidized bed experiment (from Ref. (Abate and Durian, 2007)).

relatively short time scale  $\tau_{jump} \simeq 10$ . The cluster size distribution is well described by a power law  $\rho(N_c) \approx N_c^{-\alpha}$  where  $N_c$  is the number of grains within a cluster and  $\alpha \in [3/2 - 2]$ . The distribution of the lag times separating two adjacent clusters exhibits an excess of small times as well as an excess of large times as compared to a Poissonian uncorrelated process, and can be described by the superposition of two distributions: one for the long times corresponding to the distribution of the time spent by the particles in each cage, and one for short delays between adjacent clusters which suggest a facilitation mechanism among clusters, the origin of which remains to be found. As a result of these two timescales, the clusters form avalanches well separated in time and space. Finally, selecting a time interval of length  $\tau_{DH}$  corresponding to the timescale for which dynamical heterogeneities are maximal, initiated at the beginning of a given avalanche, Fig. 0.4-rhs displays the spatial organization of the clusters in the avalanche. One can see how the clusters spread and built up a region of identical temporal decorrelation and thereby conclude that the avalanches are the dynamical heterogeneities.

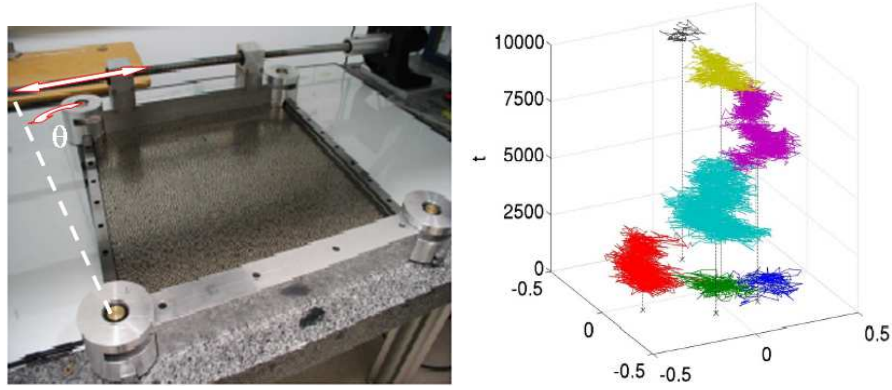


**Fig. 0.3** The cyclic shear cell experiment (from Ref. (Marty and Dauchot, 2005)). A bi-dimensional, bi-disperse granular material, composed of about 8,000 metallic cylinders of diameter 5 and 6 mm in equal proportions, is sheared quasi-statically in an horizontal deformable parallelogram. The shear is periodic, with an amplitude  $\theta_{max} = \pm 5^\circ$ . The volume accessible to the grains is maintained constant by imposing the height of the parallelogram, so that the volume fraction is a constant ( $\phi \simeq 0.84$ ). Up to 4000 grains located in the center of the device are tracked by a High Resolution Digital Camera which takes a picture each time the system is back to its initial position  $\theta = 0^\circ$ . The unit of time is then one cycle, one experimental run lasting 10,000 cycles. The unit of length is chosen to be the small particle diameter  $d$ . Images are taken at each cycle and the resulting stroboscopic trajectories of the grains exhibit typical cages separated by cage jumps (rhs).

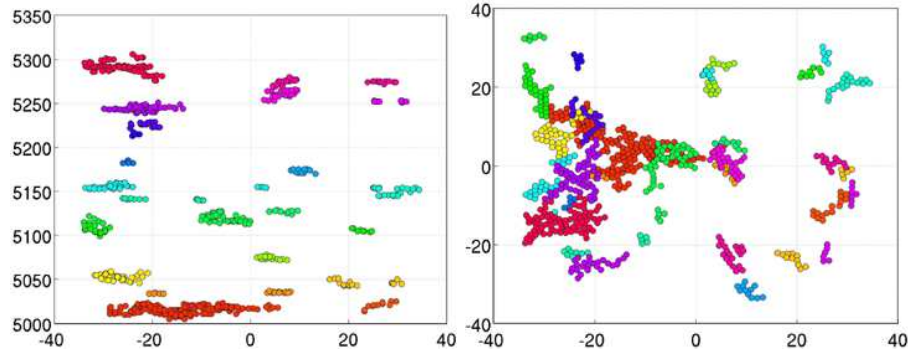


**Fig. 0.4** Spatio-temporal organization of the cage jumps (from Ref. (Candelier *et al.*, 2009a)). Left: Time of cage jump (vertical axis) vs its x-coordinate (horizontal axis). Right: Spatial location of cage jumps, showing that cage jumps facilitate each other to form dynamical heterogeneities.

Theoretical approaches based on dynamic facilitation usually focus on kinetically constrained models (Ritort and Sollich, 2003; Garrahan and Chandler, 2002; Toninelli *et al.*, 2006). They are characterized by a common mechanism leading to slow dynamics: relaxation



is due to mobile facilitating regions that are rare and move slowly across the system. Here, we find a dynamics characterized by avalanches inside which clusters are facilitating each other. However, in the present system facilitation is not conserved as in kinetically constrained models since the first cluster of an avalanche is far from any other possible facilitating region. Recent observations (Candelier *et al.*, 2009b) in the fluidized bed experiment described in the previous section confirm that indeed facilitation becomes less and less conserved and a less and less significant mechanism when approaching jamming. Also it has been shown numerically that the mechanisms described in this section also hold in a repulsive supercooled liquid (Candelier *et al.*, 2009c). This is a remarkable fact given the fundamental difference between the athermal granular system and the thermal structural liquid.

### 0.2.3 Criticality across the jamming transition

Once the system has entered the glass phase, its relaxation time has become much larger than the experimental timescale and it has fallen off equilibrium. However, one can still increase the packing fraction under external vibration, up to some value, where a finite fraction of particles will need to overlap to accommodate the increase of packing fraction. At that point, the pressure feels the hardcore repulsion of the grains and jamming occurs.

Lechenault *et al.* considered the dynamics of a bidisperse monolayer of disks under horizontal vibration (Lechenault *et al.*, 2008a) — see Fig. 0.5. The quench protocol produces reproducible, very dense configurations with structural relaxation time  $\tau_\alpha$  much larger than the experimental time scales. The pressure in the absence of vibration falls to zero at the jamming transition  $\phi_J \in [0.8417, 0.8422]$ , and in this system the density can be increased beyond this transition. One then observes that long-time correlations, accompanied by the growth of spatial correlations, are maximal at  $\phi_J$ . Here a snapshot of the displacement field reveals the existence of a super-diffusive motion organized in channel currents meandering between blobs of blocked particles.

Figure 0.5-rhs displays the root mean square displacement as a function of the lag  $\tau$  for various packing fractions  $\phi$ . The very small values of  $\sigma_\phi(\tau)$  at all timescales are consistent with the idea that the packing remains in a given structural arrangement. At low packing fractions  $\phi < \phi_J$ , and at small  $\tau$  the mean square displacement displays a sub-diffusive behavior before recovering a diffusive regime at longer timescales. As the packing fraction is increased, the typical lag at which this cross-over occurs becomes larger and, at first sight, does not seem to exhibit any special feature for  $\phi \simeq \phi_J$ . Above  $\phi_J$ , an intermediate plateau appears before diffusion resumes. A closer inspection of  $\sigma_\phi^2(\tau)$  reveals an intriguing behavior, that appears more clearly on the local logarithmic slope  $\nu = \partial \log \sigma_\phi(\tau) / \partial \log(\tau)$  (see (Lechenault *et al.*, 2008a; Lechenault *et al.*, 2008b)). For packing fractions close to  $\phi_J$  and after the sub-diffusive regime, the motion becomes *super-diffusive* at intermediate times corresponding to large scale currents shown in figure 0.6-(a).

To characterize the various diffusion regimes, these authors define three characteristic times:  $\tau_1(\phi)$  as the lag at which  $\nu(\tau)$  first reaches  $1/2$ , corresponding to the start of the super-diffusive regime,  $\tau_{sD}(\phi)$  when  $\nu(\tau)$  reaches a maximum  $\nu^*(\phi)$  (peak of super-diffusive regime), and  $\tau_D(\phi)$  beyond which the system recovers the diffusive

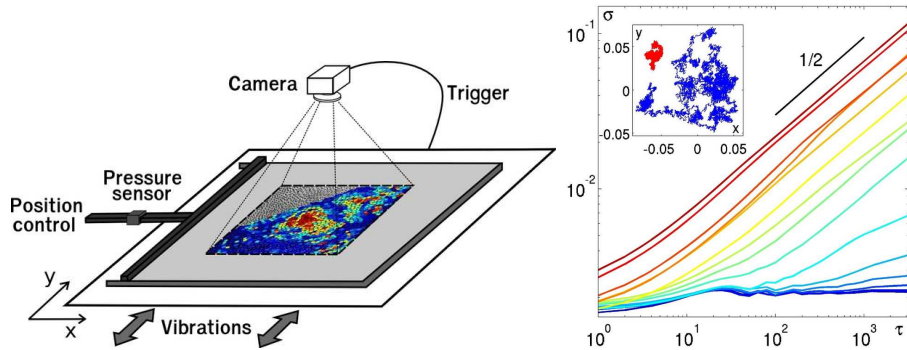


**Fig. 0.5** A monolayer of bi-disperse grains is driven close to jamming by successive compression steps under horizontal vibration (from Ref. (Lechenault *et al.*, 2008a)). Left: Set up. A bidisperse monolayer of 8500 brass cylinders of diameters  $d_{small} = 4 \pm 0.01\text{mm}$  and  $d_{big} = 5 \pm 0.01\text{mm}$  laid out on a horizontally vibrated glass plate (frequency : 10Hz, amplitude : 10mm). A lateral mobile wall allows to vary the packing fraction by tiny amounts ( $\delta\phi/\phi \sim 5 \cdot 10^{-4}$ ) within an accuracy of  $10^{-4}$ . The pressure exerted on this wall is measured by a force sensor inserted between the wall and the stage. The stroboscopic motion – in phase with the oscillating plate – of a set of 1500 grains in the center of the sample is tracked by a CCD camera. Lengths are measured in  $d_{small}$  units and time in cycle units. Right: the root mean square displacements exhibits a strongly subdiffusive behaviour at short time before recovering diffusive motion. Note that even for the loosest packing fraction, the total displacement on the duration of the experiment does not exceed 0.1 grain diameter. The inset shows two trajectories, in blue for the loosest packing fraction, in red for the highest ones

regime. These characteristic time scales are plotted as a function of the packing fraction in Fig. 0.6-(b). Whereas  $\tau_1$  does not exhibit any special features across  $\phi_J$ , both  $\tau_{sD}$  and  $\tau_D$  are strongly peaked at  $\phi_J$ .

Finally, one can extract the typical size of these currents by computing the dynamical susceptibility  $\chi_4(\tau)$ , which quantifies the number of particles moving in a correlated manner and exhibits a maximum at  $\tau^*$ . Interestingly  $\tau^*$  behaves like  $\tau_{sD}$ , a further proof that in the present case, super-diffusion and dynamical heterogeneities are related. Recently a deeper analysis of the same data have revealed that the super-diffusive behaviour must be attributed to the emergence of Levy-flights in the displacement distributions rather than to long time correlations, suggesting the existence of rapid cracks of all scales rather than the progressive development of soft regions (Lechenault *et al.*, 2010).

Another way to characterize the spatial correlation is to compute the spatial correlator of the displacement field amplitude for a lag  $\tau^*$  (see appendix). The authors could demonstrate that this spatial correlator also called four-point correlation function obeys critical scaling  $G_4(\vec{r}, \tau^*) \propto \frac{1}{r^\alpha} \mathcal{G}\left(\frac{r}{\xi_4}\right)$ , with  $\alpha \simeq 0.15$  in the vicinity of  $\phi_J$ .  $\xi_4(\phi)$ , plotted on Fig.0.6-(c), is the length scale over which dynamical correlations develop. This scaling form, together with the strong increase of both  $\xi_4(\phi)$  and  $\tau_{sD}(\phi)$

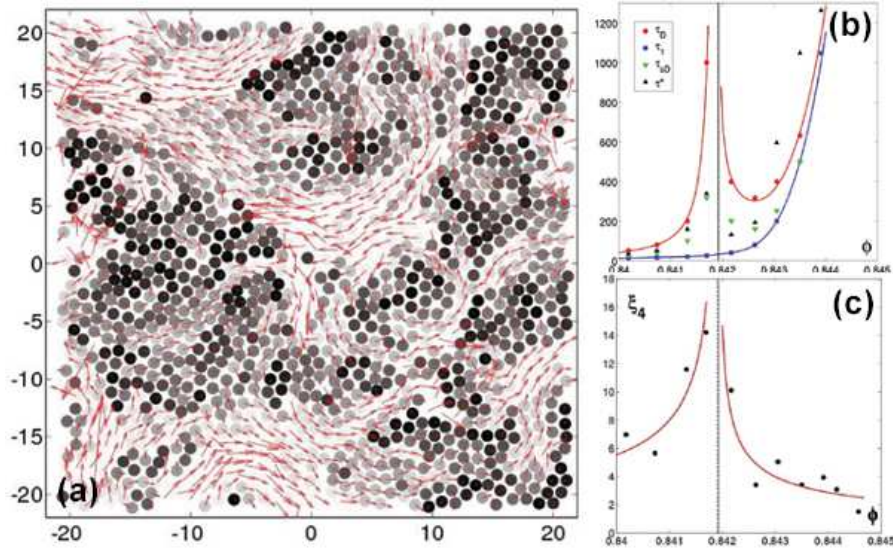


**Fig. 0.6** Criticality at jamming (from Ref. (Lechenault *et al.*, 2008a)): displacements on time-scale  $\tau^*$  (b) are the most heterogeneous ones; they correspond to super-diffusive currents of correlated particles (a), which develop on a length scale  $\xi_4$  (c), which strongly increases on both side of the transition. The time-scale needed to recover normal diffusion  $\tau_D$  (b) exhibits the same sharp peak at the transition. NB: the displacements have been magnified by a factor of 50. The color code is black (resp red) for the less mobile (resp the fastest) particle.

over a minute range of  $\phi$ , is the strongest evidence that the jamming fraction  $\phi_J$  is indeed a critical point, where a static pressure appears *and* long-range dynamical correlations develop.

### 0.3 Heterogeneities in granular flows

#### 0.3.1 Flow Rules

Three different granular flow regimes are to be distinguished. *Rapid flows* are fairly dilute. The main grain interactions are through collisions, and this regime is described well within the framework of the kinetic theory (Savage and Jeffrey, 1981; Goldhirsch, 2003). *Slow flows* are dense, and the grain interactions are dominated by the frictional contact forces. This is the regime associated with soil mechanics (Nedderman, 1992), although existing descriptions for such slow flows are rather incomplete and have limited predictive power (Fenistein *et al.*, 2004; Deboeuf *et al.*, 2005). *Liquid-like granular flows* constitute the intermediate regime, where both inertia and friction are important and grain interactions are a mix between enduring contacts and collisions. This last regime has been widely investigated recently (MiDi, 2004; Savage, 1998; Losert *et al.*, 2000; Mills *et al.*, 1999; Aranson and Tsimring, 2002; Cortet *et al.*, 2009; Lemaître, 2002; Deboeuf *et al.*, 2006).

The crucial progress made recently comes from dimensional analysis (Iordanoff and Khonsari, 2004; MiDi, 2004; da Cruz *et al.*, 2005) which suggests that, in simple incompressible uni-

directional uniformly sheared flows, there is only one dimensionless number which governs the flow: the so-called *Inertial Number*  $I = \dot{\gamma}d/\sqrt{P/\rho}$ , which is a function of bead diameter  $d$ , grain density  $\rho$ , global pressure  $P$  and global shear rate  $\dot{\gamma}$ . The rheology is then set by requiring that the ratio of shear to normal stresses is given by an effective friction coefficient which depends on the inertial number only:  $\tau/P = \mu(I)$ . Such relation has first been evidenced, numerically, in plane shear (Iordanoff and Khonsari, 2004; da Cruz *et al.*, 2005) and, experimentally, in inclined plane (MiDi, 2004) configurations. A local tensorial extension of this relation was recently proposed by Jop *et al.* (Jop *et al.*, 2006) as a constitutive law for dense granular flows, and these authors succeeded to fit the surface velocity profile for a steady unidirectional flow down an inclined plane with walls. Microscopically, it has been proposed by Ertas and Halsey (Ertas and Halsey, 2002) that the motion of grains in dense granular flows occurs through clusters, whose size is controlled by the stress distribution. In the remainder of this section we will focus now on heterogeneities arising in this flow regime.

### 0.3.2 Granular Flows in Rotating Drums

Pouliquen (Pouliquen *et al.*, 2003) has experimentally studied the velocity fluctuations of grains flowing down a rough inclined plane. He has shown that grains at the free surface exhibit fluctuating motions, which are correlated over a few grain diameters. Surprisingly, the correlation length is not controlled by the thickness of the flowing layer but by the inclination only. The correlation length is maximum at low inclination and decreases at high inclination, in a similar way as the critical thickness below which, for a given inclination, the flow stops (Daerr and Douady, 1999).

Bonamy *et al.* (Bonamy *et al.*, 2002) have also observed clusters of particles in the steady flow regime in a rotating drum. In the recorded region, located at the center of the drum, the granular surface flow presents the now well known velocity profile, linear in the flowing surface flow and exponential in the quasi-static bed (see Fig. 0.7-b). By tracking the particles Bonamy *et al.* found that the velocity fluctuations of two beads in contact tend to have correlated orientations. Figure 0.7(c) displays the resulting clusters — here clusters are defined as consisting of particles in contact with velocity fluctuations aligned to within  $60^\circ$ . The authors further showed that the distribution of the number of beads in a cluster is a power law with a cut-off given by the flow thickness, thereby enforcing an earlier scenario proposed by Ertas and Halsey (Ertas and Halsey, 2002).

What are the timescales governing these spatially correlated clusters? Deboeuf *et al.* (Deboeuf *et al.*, 2003) studied the related question of the typical relaxation times of the granular assembly inside the drum, once the flow is stopped. For that purpose the drum is first rotated in the well known regime of intermittent avalanches, and then stopped just after an avalanche has occurred. The subsequent relaxation events are then recorded with a standard CCD camera, which takes images of the pile every 15 s. Denoting the fraction of beads that have moved between two acquisitions by  $\delta A(t)$ , the slow relaxation of the pile can be characterized.

Two qualitatively different types of behavior can be found, as illustrated in Fig. 0.8. During the very first time steps the relaxation process is identical in both records: the

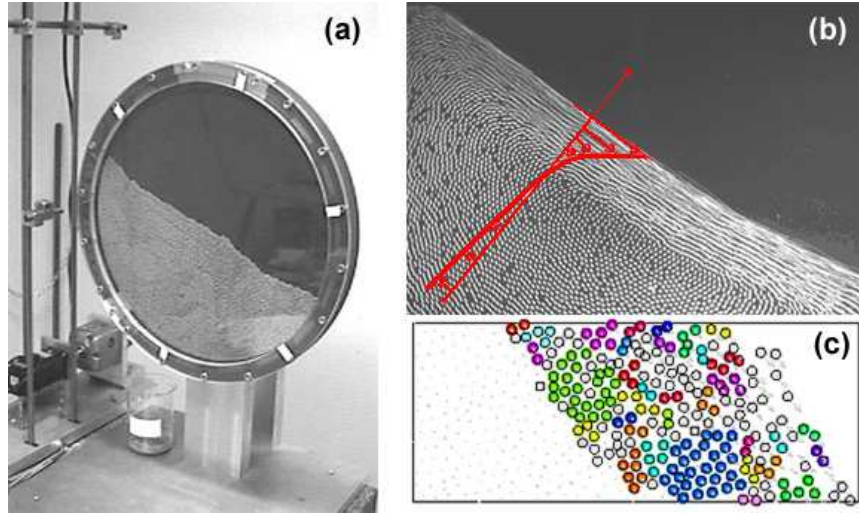


**Fig. 0.7** Rotating drum experiment (from Ref. (Bonamy *et al.*, 2002)). (a) Set up consisting of a rotating drum of diameter 45 cm and gap of 7 mm, half filled with steel beads of diameter  $d = 3 \pm 0.05$  mm. A quasi-2D packing is obtained but with a local 3D microscopic disordered structure. A fast camera allows to track the 60 percents of the beads observed through the transparent side wall of the tumbler. The rotating velocity of the drum is varied from 1 rpm to 8 rpm. (b) Linear (resp. exponential) velocity profile in the upper flowing layer (respectively the lower static layer). (c) Clusters of beads with correlated velocity fluctuation orientation in quasi 2D flow; typical frame of the clusters for  $\Omega = 8rpm$

bulk of the pile relaxes rapidly from bottom to top on time-scales of the order of 15 s — typical events involve isolated bead displacements on short time and length scales. The relaxation process then slows down in a subsurface layer of thickness  $[10 - 20]$  bead diameters — this subsurface layer may relax very differently from one realization to another (see fig. 0.8).

In one case, one observes a simple exponential decay of the subsurface layer activity with a characteristic timescale of the order of 200 seconds. In the other case, intermittent bursts interrupt periods of exponential decay, with the same time-scale as in first case (see inset of Fig. 0.8-lhs). The competition between the exponential relaxation and the reactivation bursts results in a much slower relaxation. A visual inspection reveals that the reactivation bursts correspond to collective motions of grain clusters whereas the exponential decay involves individual bead displacements — see Fig. 0.8-rhs. For the case of burst events those displacements persist in time and are spatially correlated, forming grain clusters.

Altogether the above experiments reveal the existence of correlated clusters, which seemingly control the thickness of the steady flow and the relaxation times of the avalanches in the intermittent regime. Such clusters are purely dynamical in the sense that they involve spatial correlations of the dynamics, not of the local structure inside the pile. A characterization of these dynamical correlations in terms of dynamical heterogeneities, as introduced for the study of glasses, has not been done in the case



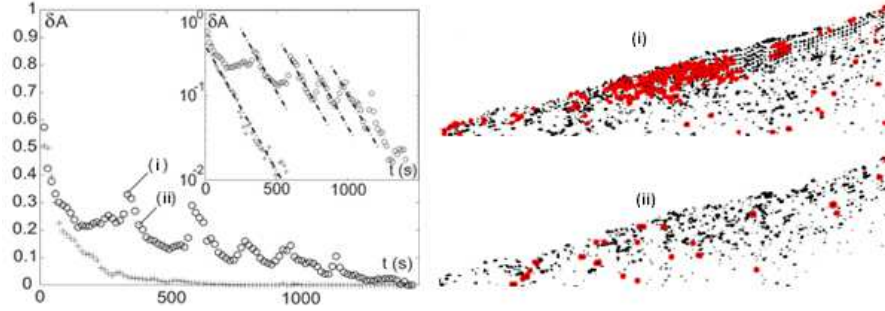


**Fig. 0.8** Intermittent relaxations following a sudden flow arrest (from Ref. (Deboeuf *et al.*, 2003): the evolution of the fraction of mobile grains  $\delta A(t)$  for two different realizations at similar pile slopes: (●)  $\theta = 15$  deg; (+)  $\theta = 16.5$  deg. Inset is the log-lin plot of the same data. Notice the exponential decay rate, which is identical in the monotonous case (+) and in the intermittent case (●). On the rhs, displacements in the pile during a burst event (i) and during an exponential decay period (ii). The dark pixels correspond to positions where a displacement has occurred in the 15 s preceding the considered time step. The red (light) overlay indicates the pixels, where displacements have occurred successively during 30 s following the given time step (see text for details).

of the rotating drum, at least not in a systematic manner, but was done for the flow down a pile, as we will discuss now.

### 0.3.3 Granular Flows down a Pile

One striking feature of granular flow down a pile is that the flow near the surface can be very smooth and fluid-like while simultaneously far below the surface the heap appears to be a completely static solid. This is true even at very high mass flux, when the surface flow is steady and independent of time. This situation has now been extensively studied in a simpler geometry where the heap is confined in the narrow gap between two transparent side walls through which the grains may be measured optically. Several groups report that the velocity profile along the sidewall decreases nearly exponentially with depth (Lemieux and Durian, 2000; Khakhar *et al.*, 2001; Komatsu *et al.*, 2001; Andreotti and Douady, 2001; Jop *et al.*, 2005; Djaoui and Crassous, 2005; Richard *et al.*, 2008). Similar localized flow behavior is found for grains in a rotating drum (Rajchenbach, 1990; du Pont *et al.*, 2005; Cortet *et al.*, 2009; MiDi, 2004), as well as in Couette (Howell *et al.*, 1999; Mueth *et al.*, 2000; Bocquet *et al.*, 2002) and split-ring (Fenistein *et al.*, 2004) cells. Due to the exponential character of the velocity profiles for continuous heap flow, the shear rate is highest near the top free surface where the velocity is highest, and it decays almost exponentially with depth, too. Thus the grains experience neighbor changes most frequently and are most unjammed near the top, and they become progressively jammed as a function of depth.

The nature of the jamming transition for continuous heap flow, controlled as a function of depth, was recently studied and compared with jamming transitions for uniform systems controlled as a more usual function of temperature or density or shear

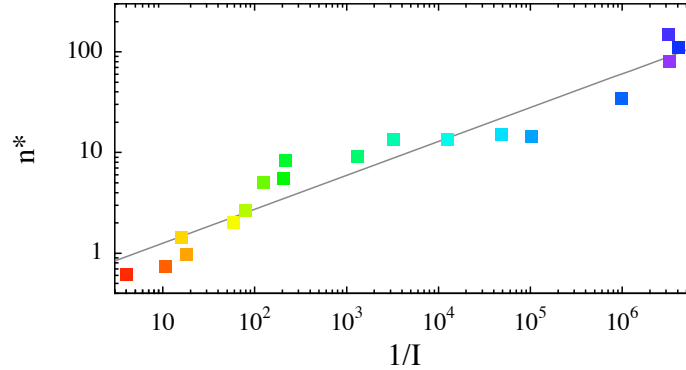


**Fig. 0.9** Number  $n^*$  of grains in a heterogeneity for heap flow versus inverse inertial number,  $I = \dot{\gamma}d/\sqrt{P/\rho}$ , where  $\dot{\gamma}$  is the shear rate,  $d$  is the grain diameter,  $P$  is the local pressure, which depends on depth, and  $\rho$  is the grain density (from Ref. (Katsuragi *et al.*, 2009)). The line is the best fit to a power-law, giving  $n^* \sim (1/I)^{0.33 \pm 0.02}$  in accord with simulation of a system undergoing uniform shear (Hatano, 2008).

(Katsuragi *et al.*, 2009). Measurement of the static structure factor and pair correlation function for grains along the sidewall show that the spatial arrangement of grains is slightly dilated in the first layer or two due to saltation. At greater depths, there is no noticeable change in structure to accompany the dramatic decreases in velocity and shear rate. Such behavior is a hallmark feature: glass and jamming transitions are dynamical, and are not controlled by the growth of a correlation length associated with instantaneous (static) order.

There are two interesting features in the dynamics that both grow with depth on approach to jamming. The first is the ratio of the characteristic grain fluctuations speed,  $\delta v$ , to the flow speed,  $v_x$ ; the former is measured by speckle-visibility spectroscopy, while the latter is measured by particle-image velocimetry (Katsuragi *et al.*, 2009). While both speeds decrease with depth, the fluctuations do so more slowly in accord with  $\delta v \propto \sqrt{v_x}$ . The relative rise of  $\delta v$  over  $v_x$  for greater depth signifies an increase in jostling and hence in dissipation at decrease driving rates, that ultimately results in jamming; it also means that the flow does not simply slow down without change in character. In particular, the second interesting feature is that the character of the dynamics becomes increasingly heterogeneous on approach to jamming. This is seen by measurement of an overlap order parameter and associated susceptibility,  $\chi_4(\tau)$ , based on a novel image correlation method that does not rely on particle tracking (Katsuragi *et al.*, 2009). At all depths,  $\chi_4(\tau)$  displays a peak vs  $\tau$  which is located very close to grain radius divided by  $v_x$ , and hence which slows to longer times at greater depths. More importantly the height of the peak,  $\chi_4^*$ , increase nearly exponentially with depth. This means that the dynamics become increasingly heterogeneous on approach to jamming.

To compare with other systems, it is more appropriate to consider the growth in the number  $n^*$  of grains in a heterogeneity as a function of shear rate rather than of

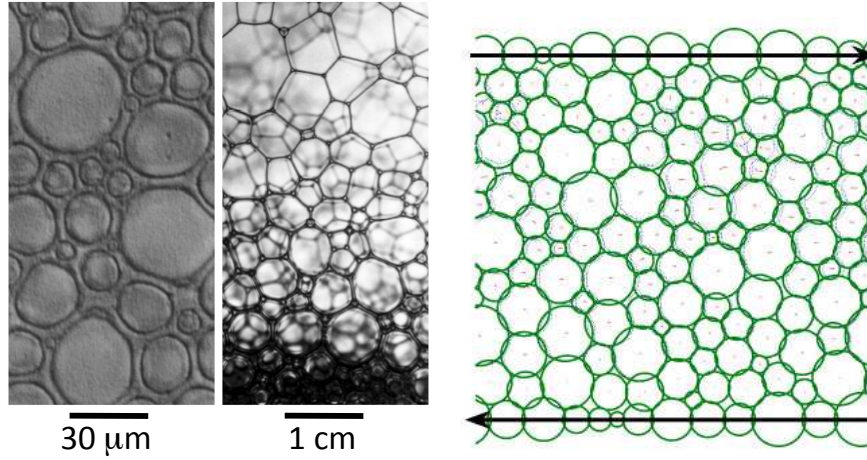


**Fig. 0.10** Left: Gas bubbles in a shaving cream and in a vial of soapy water about 30 minutes after shaking. The former is about 92% gas, while the latter has a vertical gradient in wetness due to gravity. Right: The bubble model as introduced in (Durian, 1995; Durian, 1997) : bubble positions just before (blue) and after (green) a shear-induced rearrangement, with trajectory of the centers shown in red

depth. For this,  $n^*$  is computed from  $\chi_4^*$  as shown in the appendix, and the shear rate is characterized by the inertial number (MiDi, 2004). For the experiment,  $I$  is maximum at about 0.2 near the surface and decays nearly exponentially with depth. The scaling displayed in Fig. 0.9 of the size of the heterogeneities with dimensionless shear rate is a power-law relation  $n^* \sim I^{-1/3}$ .

#### 0.4 Foams, frictionless soft spheres

Foams are dispersions of gas bubbles in liquid, stabilized by surfactants (Fig. 0.10-left) (Kraynik, 1988; Wilson, 1989; Prud'homme and Khan, 1996; Weaire and Hutzler, 1999). A crucial parameter is the liquid fraction, or wetness of the foam, which specifies the volume fraction of the liquid phase. When the liquid fraction is too large, the individual gas bubbles do not touch and the material is unjammed — one refers to this as a bubbly liquid rather than a foam. Below a critical liquid fraction — around 36% percent for 3d foams — bubbles can no longer avoid each other and undergo a jamming transition. What is particular for foams is that vanishingly small liquid fractions can easily be reached, where the foam essentially consists of very thin liquid layers meeting in quasi 1D plateaux borders, which themselves meet in vertices — such foams are called dry foams. In systems under gravity, drainage can cause gradients in the wetness from very dry at the top to wet at the bottom.

It is interesting to compare bubbles in foam with grains in a sandpile. In common, both are comprised of large packing units which experience negligible thermal motion and which tend to be jammed. But there are many contrasts: First, grains in a pile are effectively incompressible, and pack at packing fractions *below* random close packing, while bubbles in a foam are readily deformed and squashed together *above* random



close packing. Second, grains are subject to static and sliding friction, as well as to collisional dissipation, whereas the bubble contacts are through a liquid film which typically does not support static friction.

This has important implications for differences between the jamming of foams and the jamming of grains. Hard grains essentially are always close to jamming, but due to the friction, they are not necessarily critical — the jamming transition for frictional particles is usually not critical, and is not characterized by a unique packing fraction or contact number (van Hecke, 2010). In contrast, the jamming transition for foams (and emulsions) has all the hallmarks of the theoretically well-studied jamming of soft frictionless spheres at point J. Here the jamming transition corresponds to a precise packing fraction and contact number, and materials near point J exhibit a diverging length-scale and non-trivial powerlaw scaling of their elastic moduli (O’Hern *et al.*, 2003a; van Hecke, 2010). Some of these features have, in fact, been discovered first in numerical simulations of simple models of foams (Bolton and Weaire, 1990; Durian, 1995; Durian, 1997) (see fig. 0.10).

Flows of granular media and foams also exhibit essential differences. Granular flow requires dilatation, and can be separated in slow and fast flow depending on the role of inertia. In contrast, foam flows are highly damped due to viscous interactions, and accomplished by bubble deformation and rearrangement with no dilatation — inertia plays essentially no role.

#### 0.4.1 Unjamming of foams

There are at least three ways to unjam foams. The first is simply to allow the foam to coarsen: with time gas will diffuse from high to low pressure bubbles, which generally causes smaller bubbles to shrink and larger ones to grow. This is driven by surface tension through Laplace’s law, and serves to reduce the total interfacial area. As coarsening proceeds, the bubbles rearrange into different packing configurations and hence can relax macroscopically-imposed stress. The time scale for rearrangement can be comparable to that for size change, as in very dry foams. But for fairly wet foams, the rearrangements can be very much faster. Such avalanche-like rearrangements are a kind of dynamical heterogeneity, where a localized region of neighboring bubbles briefly mobilizes and comes to rest in a new configuration. For opaque foams, these events may be captured by diffusing-wave spectroscopy and its variants (Durian *et al.*, 1991; Cohen-Addad and Hohler, 2001; Gittings and Durian, 2006). The measured signal gives the time between successive rearrangements at a scattering site, averaged over both time and the volume of the sample through which the photons diffuse. As the foam coarsens, the time between events is found to grow as a power-law of time. The DWS signal also includes subtle contributions from continuous motion of the gas-liquid interfaces, due to both thermal fluctuations (Gopal and Durian, 1997) and also the coarsening process (Gittings and Durian, 2008; Sessoms *et al.*, 2010).

Time-resolved versions of DWS allow further information to be extracted (see fig. 0.11). In Ref. (Mayer *et al.*, 2004),  $\chi_4(\tau)$  is measured by fluctuations in the decay-rate of the DWS correlation function. As the foam coarsens, the peak location moves to longer times in accord with the growing time between events. Furthermore, the peak height also grows – perhaps because the scattering volume contains a decreasing num-

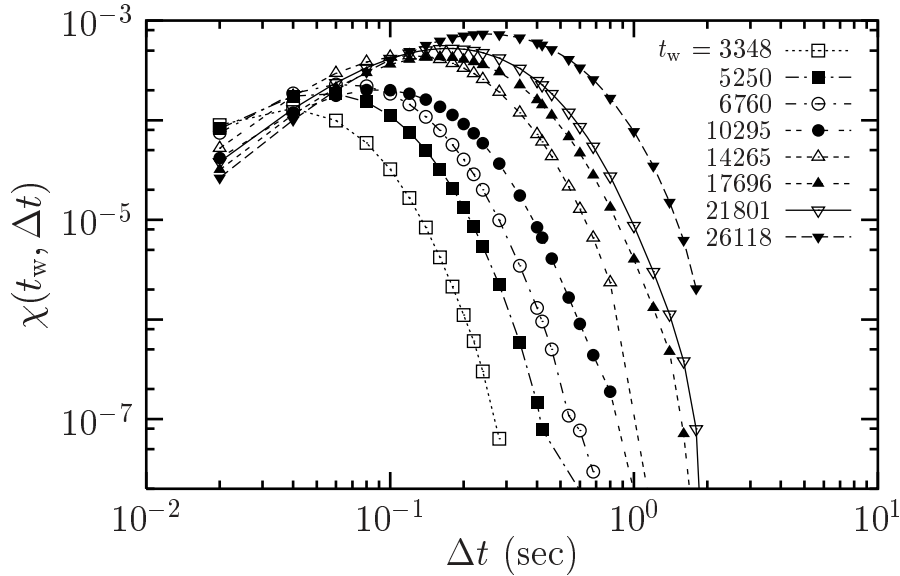


**Fig. 0.11** Dynamical susceptibility measured by light scattering for a coarsening foam at different wait times  $t_w$ , labeled in seconds (Mayer *et al.*, 2004). Note that the peaks shifts to longer times and grows in height as the foam ages.

ber of bubbles and perhaps because the system is becoming progressively jammed. In Ref. (Gittings and Durian, 2008), the scattering volume is decreased to the point that the dynamics of individual rearrangements may be followed with speckle-visibility spectroscopy. This allows access to a second important timescale – the *duration* of the rearrangement events. In addition, the spatial distribution of successive events may now be studied with a recently introduced photon correlation imaging technique (Duri *et al.*, 2009; Sessoms *et al.*, 2010).

Foams may also be unjammed by application of shear. As probed by DWS (Earnshaw and Jaafar, 1994; Gopal and Durian, 1995), the shear-induced rearrangements appear similar to the coarsening-induced rearrangements but occur at frequency proportional to the strain rate. So coarsening dominates at very low strain rates, small compared to the reciprocal of the time between coarsening-induced events. At very high strain rates, compared to the reciprocal of the *duration* of events, the bubble-scale dynamics are qualitatively different. Rearranging bubbles no longer have enough time to lock into a locally-stable configuration before having to rearrange again. Thus successive events merge into continuous flow, and bubble-bubble interactions are dominated by dissipative forces rather than surface-tension forces. This is evidenced by a change in the functional form of the DWS correlation function (Gopal and Durian, 1999), similar to the change due to diffusive vs ballistic microscopic motion. The effect of altered microscopic dynamics on the macroscopic rheology may be seen to some extent in the shape of the stress vs strain rate flow curve; however, it is much more apparent in the transient stress jump and decay observed when a small step-strain is superposed on steady shear (Gopal and Durian, 2003). In particular, the transient shear modulus

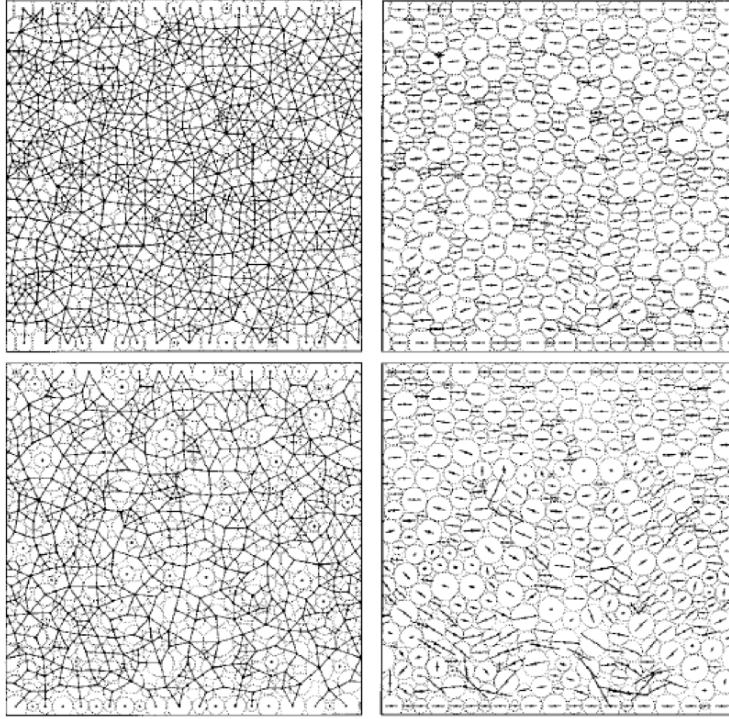


**Fig. 0.12** Bubble positions and spring network (left column), for the model of Refs. (Durian, 1995; Durian, 1997). The top row is for a packing fraction of 1 and the bottom row is for a packing fraction of 0.84. The right column depicts the motion that occurs for small-amplitude shear strain, showing that it becomes more nonaffine on approach to unjamming.

and stress relaxation time both decrease vs strain rate at a characteristic scale set by yield strain divided by event duration (Gopal and Durian, 2003).

Finally, the third approach to unjam foams is by increasing the liquid content. In the dry limit, the bubbles are polyhedral and separated from their neighbors by thin curved soap films. The addition of liquid causes inflation not of the films but of the Plateau borders and vertices at which the films meet. Thus progressively wetter foams have progressively rounder bubbles, which unjam when the liquid fraction rises to about 36% and the bubbles are randomly close-packed spheres filling about 64% of space (in 3d). This unjamming has been measured in terms of the vanishing of the shear modulus and the yield strain vs liquid fraction (Saint-Jalmes and Durian, 1999). While rearrangements play no role in this transition, there is nonetheless interesting changes in dynamics. First, as seen in simulation, there is a growing time scale for stress relaxation (Durian, 1995). This is accompanied by, and in fact may be due to, bubble displacements that become increasingly non-affine as the liquid fraction ap-

proaches unjamming (Durian, 1997) as illustrated on fig. 0.12. Non-affine response has been implicated in a  $\sqrt{i\omega}$  contribution to the complex shear modulus (Liu *et al.*, 1996; Gopal and Durian, 2003), and in the non-trivial scaling of the shear modulus with packing fraction (O'Hern *et al.*, 2003b; Ellenbroek *et al.*, 2009).

#### 0.4.2 Flow of 2D foams

Experiments on two-dimensional foam under shear have yielded tremendous insight, in part because the full bubble-packing structure can be readily imaged and tracked as a function of time but also because the dry limit may be modeled in terms of idealized topological features (Bolton and Weaire, 1990; Herdtle and Aref, 1992; Okuzono and Kawasaki, 1995). Pioneering measurements on shear bubble rafts date back to Argon (Argon and Kuo, 1979), who sought analogy with the flow of metallic glasses.

In recent years, a variety of studies have addressed the flow of quasi-2D foams, which consist of a single layer of macroscopic ( $d > 1mm$ ) bubbles. Such single layers can be made by freely floating bubbles on the surface of a surfactant solution (Y. H. Wang, 2006), by trapping them between a top glass plate and the surfactant solution (G. Katgert and van Hecke, 2008; Y. H. Wang, 2006), or by trapping them between two parallel glass plates (G. Debregeas and di Meglio, 2001). The confining glass plates enhance the stability of the foam, but also introduce additional drag forces that lead to the formation of shear bands in the foam (Y. H. Wang, 2006).

While the time-averaged flow profiles in such geometries have received much attention (G. Debregeas and di Meglio, 2001; Lauridsen *et al.*, 2004; Y. H. Wang, 2006; E. Janiaud and Hutzler, 2006; G. Katgert and van Hecke, 2008) here we will briefly outline recent work on the fluctuations around the average flows. As shown by Debregeas (G. Debregeas and di Meglio, 2001) and Lauridsen *et al.* (Lauridsen *et al.*, 2004), the instantaneous flow field exhibits swirly, vortex like motion, commonly observed in other flowing systems near jamming also. Moreover, T1 events (local changes in the contact topology) are readily observed in these systems (Lauridsen *et al.*, 2004; Y. H. Wang, 2006).

The probability distributions describing the instantaneous bubble velocities exhibit fat tails (Wang *et al.*, 2006). Consistent with this, Möbius *et al.* established that, for a given local strain rate, the probability distributions of bubble displacements exhibit fat tails for short times, develop exponential tails for intermediate times and finally become Gaussian. The occurrence of purely exponential distributions at a sharply defined time defines the relaxation time  $t_r$ , which coincides with the crossover time from super diffusive to diffusive behavior, and also with the Lindeman criterion (M.E. Möbius and van Hecke, 2008).

Surprisingly,  $t_r$  is not proportional to the inverse of the strain rate which would be the simplest relation consistent with dimensional arguments, but instead exhibits a non-linear relationship with the strain rate. This has a direct consequence for the probability distributions of bubble displacements taken at a fixed strain: the width of this distribution grows as  $\dot{\gamma} \rightarrow 0$ . This so-called sub-linear scaling, which has been observed in simulations (I. K. Ono and Liu, 2003), implies that these flows are not quasi-static, but rather that the amount of fluctuations increases for slower flows — not dissimilar to what we discussed above for granular pile flows.

For collections of viscous bubbles with known bubble-bubble interactions, the balance of work done on the system and the energy dissipated at the local scale, immediately dictates this sub-linear scaling (I. K. Ono and Liu, 2003; B. Tighe and van Hecke, 2010). It has recently been suggested by Tighe *et al* that the nontrivial scaling of the fluctuations also governs the non trivial rheology of foams — where the global relation between strain rate and stress does not follow directly from the local relation between relative bubble motion and drag forces (Olsson and Teitel, 2007; G. Katgert and van Hecke, 2008; B. Tighe and van Hecke, 2010). This provides an intriguing link between non trivial behavior at micro and macro scale — how the spatial organization of the strong bubble fluctuations associated with sub-linear scaling connects to dynamical heterogeneities in foams is at present an important open question.

## 0.5 Discussion

We have discussed the heterogeneities that arise in a variety of weakly driven systems near jamming. These heterogeneities have unveiled the existence of a dynamical length-scale and the associated timescale responsible for the slow relaxation of these systems. On one hand the existence of such a lengthscale can be argued to be at the origin of the quasi-universal behaviour observed in these glassy systems. On the other hand the observed lengthscale is always rather small, say smaller than 10 particles diameters and the effect of the different microscopic mechanisms may still be significant.

For example, for the fluidized grains, interactions are mainly collisional, for the dense grain systems across the jamming transition they are mainly frictional, for the pile flows they are a combination of collisions and enduring contacts, while for foams the interactions are viscous.

Another important difference between these systems is that different sets of coordinates can be expected to characterize their states. For example, the structure of collisional grains is set by their positions only, and structural relaxation will be related to real space motion and cage breaking, while for dense granular assemblies that do not show substantial motion of the grains, the relevant degrees of freedom may be the contact forces, and relaxations may not be dominated by particle motion but rather by changes in the contact forces.

The microscopic mechanism of dissipation, which differs between these systems, may also play an important role. All energy fed into these systems by shear or agitations needs to be dissipated by relative motion of neighboring particles. Energy balance then may lead to the so-called sublinear scaling of fluctuations (I. K. Ono and Liu, 2003) — the details of the energy dissipation then actually set the width of the distributions characterizing the fluctuations. Is it also responsible for the spatial organisation of these fluctuations? More work is needed to clarify this.

As a matter of fact, while it is rather obvious that in dense systems, local rearrangements will couple to neighboring particles, it is far from clear what mechanism governs the spatial organization of these relaxation events. On one hand it is tempting, following recent work (Wyart, 2005; Brito and Wyart, 2006), to conjecture that the correlated currents observed here are related to the extended *soft modes* that appear when the system loses or acquires rigidity near jamming. Under the action of a mechanical drive the system should fail along these soft modes. On the other hand

recent investigations (Lechenault *et al.*, 2010) suggest that motion of frictional grains in the vicinity of the jamming transition can be interpreted as micro-crack events on all scales undermining the usefulness of harmonic modes as a way to rationalize the dynamics.

Finally, the nature of the relation, if any, between the rheological response of the materials and the dynamical heterogeneities is far from being understood. Whether the emergence of a large length scale near jamming controls the rheology is still a matter of debate. It is also possible that the answer to this question is different on both side of the transition. Further studies in this matter, including non-linear rheology and local probe experiments (Habdas *et al.*, 2004; Dollet *et al.*, 2005; Geng and Behringer, 2005; Candelier and Dauchot, 2009) will certainly contribute to uncover new and probably unexpected effects in this exciting field of soft matter physics.

## 0.6 Appendix: How to measure $\chi_4$ , and the dangers

The dynamic susceptibility  $\chi_4(l, \tau)$  has emerged as a powerful statistical tool for characterizing dynamical heterogeneities (Sillescu, 1999; Ediger, 2000; Glotzer, 2000; Lacevic *et al.*, 2003; Cipelletti and Ramos, 2005). However, its definition is somewhat involved and there are pitfalls that must be recognized and avoided if physical meaning is to be extracted from its use. We offer the following guide to help in this regard.

The first ingredient is an ensemble-averaged dynamical self-overlap order parameter,  $Q_t(l, \tau)$ , defined such that the contribution from each particle  $p$   $Q_{p,t}(l, \tau)$  is some function that decays vs delay time  $\tau$  from one to zero as the particle moves a characteristic distance  $l$  away from its location at time  $t$ . At very short (respectively very large)  $\tau$  all particles have moved a distance much less (respectively much larger) than the length  $l$  and their contribution to  $Q_t(l, \tau)$  is very nearly 1 (respectively nearly 0) with little variance for different start times. By contrast, at intermediate  $\tau$  when particles in mobile regions have moved more than  $l$  and immobile regions have moved less than  $l$ , fluctuations in the number of mobile regions cause  $Q_t(l, \tau)$  to vary noticeably around its average. In essence, the role of  $\chi_4(l, \tau) \equiv N \text{Var}(Q_t)$  is thus to capture fluctuations in the number of fast-moving mobile regions. Therefore, as shown in Fig. 0.2,  $\chi_4(l, \tau)$  vs  $\tau$  is generally expected to rise from zero to a peak at delay time  $\tau^*$  when the typical displacement is near  $l$  and then decay back to zero.

For the purpose of clarification, let us first introduce a simplified picture of a system of  $N$  particles with a fluctuating number  $M_t$  of mobile regions of size  $n$  and assume that the order parameter is  $Q_0$  in all fast regions and  $Q_1$  in slow regions. Then the order parameter is given by a weighted average of these values over the total number  $nM_t$  of particles in the fast regions and the number  $N - nM_t$  of particles in the slow regions:  $Q_t = [f_t Q_0 + (1 - f_t) Q_1]$ , where  $f_t = nM_t/N$  is the fraction of mobile particles. From this one readily obtains the averaged control parameter and  $\chi_4$ :

$$\bar{Q} = \bar{f} \delta Q + Q_1, \quad (0.1)$$

$$\chi_4 = N \text{Var}(Q) = n \bar{f} \delta Q^2 \text{Var}(M)/M, \quad (0.2)$$

where  $\delta Q = Q_1 - Q_0$  is a measure of how different are fast and slow particles. If one assumes that there is a large number of mobile regions and that they are decorrelated,



then  $\text{Var}(M) \sim M$  and one can in principle measure the size  $n$  of these regions from the above relations.

We now use the above expressions to discuss the precise way of implementing the above procedure.

#### *Choice of the order parameter:*

Most simply, it may be taken as the average over particles of step functions that drops discontinuously from one to zero when a particle moves a distance  $l$  (Glotzer, 2000; Lacevic *et al.*, 2003; Keys *et al.*, 2007). A smooth Gaussian cutoff may also be used (Marty and Dauchot, 2005; Dauchot *et al.*, 2005); then the order parameter appears like a dynamic structure factor, which motivates calling  $\chi_4(l, \tau)$  a dynamical susceptibility. The advantage of these two choices is that  $l$  may then be adjusted according to the relevant physics. For example,  $l$  approximately equal to particle radius is appropriate for the usual caging where a totally new configuration is obtained when the particles move about a particle size. Alternative choices have been made in which the cut-off length  $l$  is set to probe the topological features of the particle arrangement: the persistent area given by the fraction of space in the same Voronoi cell, and the persistent bond given by the fraction of Voronoi neighbors that remain, after a delay time  $\tau$  (Abate and Durian, 2007). But for a compressed pack of particles subject to shaking / shearing, a totally new configuration of frictional contacts arises without change in neighbors; then, a much smaller value of  $l$  is appropriate (Lechenault *et al.*, 2008a). One can also fix  $l$  on the basis of the crosscorrelation of grayscale images (Katsuragi *et al.*, 2009). When in doubt, it is useful to consider the full behavior of  $\chi_4(l, \tau)$  vs both  $l$  and  $\tau$  (Lechenault *et al.*, 2008a).

#### *Dependence on the packing fraction*

As soon as one is interested in the dependence of the size of the mobile regions at the peak of  $\chi_4$ ,  $n^*$ , on the packing fraction  $\phi$ , one should (i) check that the relevant lengthscale  $l$  does not vary too much with  $\phi$ , which is usually the case, (ii) properly normalize  $\chi_4$  by  $\bar{f}\delta Q^2$ , since the difference in mobility between the fast and the slow particles may well vary with the packing fraction too.

#### *Finite size effects*

As stated above, it is necessary to have a large enough number of independant mobile regions in order to ensure  $\text{var}(M) \sim M$ . Since one also expects large values of  $n^*$  close to the transition of interest, satisfying the above condition requires the use of very large systems, typically of the order of  $N = 100 n^*$ . These size effects rapidly become critical since the relative error on the measure of  $\text{var}(Q)$  scales like  $\sqrt{N/T}$ , where  $T$  is the duration of the acquisition.

One sees that an educated use of  $\chi_4$  requires the knowledge of both  $\delta_Q$  and  $\bar{f}$ , or equivalently the knowledge not only of the ensemble-averaged  $Q_t(l, \tau)$ , but of all individuals  $Q_{p,t}(l, \tau)$ . Clearly this is not always the case, and one can already have some insights in the dynamical heterogenities following the above procedure, but keeping in mind the caveats we have just listed. However, when one has the possibility of tracking

the particles and thereby has a direct access to the local dynamics, the dynamical heterogeneities are more precisely characterized by calculating directly the spatial correlation of the dynamics, namely the four-point correlator  $G_4(r, l, \tau)$ :

$$G_4(r, l, \tau) = \langle Q_{p,t}(l, \tau) Q_{p',t}(l, \tau) \rangle_{d_{p,p'}=r} - \langle Q_t(l, \tau) \rangle^2, \quad (0.3)$$

where  $\langle . \rangle_{d_{p,p'}=r}$  means that the average is computed over all pairs of particles separated by the distance  $r$ . The typical lengthscale of the dynamical heterogeneities  $\xi_4$  is then readily obtained from the spatial dependance of this correlator. Obviously computing  $G_4(r, l, \tau)$  is a more intensive task than the computation of  $\chi_4$ .



# References

- Abate, A. R. and Durian, D. J. (2006). *Physical Review E*, **74**(3), 031308.
- Abate, A. R. and Durian, D. J. (2007). *Phys. Rev. E*, **76**(2), 021306.
- Andreotti, B. and Douady, S. (2001). *Phys. Rev. E*, **63**(3), 031305.
- Aranson, I.S. and Tsimring, L.S. (2002). *Physical Review E*, **65**(6), 61303.
- Aranson, I. S. and Tsimring, L. S. (2006). *Rev. Mod. Phys.*, **78**, 641.
- Argon, A. S. and Kuo, H. Y. (1979). *Materials Science and Engineering*, **39**(1), 101–109.
- B. Tighe, E. Woldhuis, J. Remmers W. van Saarloos and van Hecke, M. (2010). *Preprint*.
- Bocquet, L., Losert, W., Schalk, D., Lubensky, T. C., and Gollub, J. P. (2002). *Phys. Rev. E*, **65**(1), 011307.
- Bolton, F. and Weaire, D. (1990). *Physical Review Letters*, **65**(27), 3449–3451.
- Bonamy, D., Daviaud, F., and Laurent, L. (2002). *Phys. Rev. Lett.*, **89**(034301-1).
- Brito, C. and Wyart, M. (2006). *Europhys. Lett.*, **76**(1), 149–155.
- Candelier, R. and Dauchot, O. (2009). *PRL (Physical Review Letters)*.
- Candelier, R., Dauchot, O., and Biroli, G. (2009a). *Ph. Rev. Lett.*, **102**(8), 088001.
- Candelier, R., Dauchot, O., and Biroli, G. (2009b). Evolution of dynamical facilitation approaching the granular glass transition. arXiv.org:0912.0472.
- Candelier, R., Widmer-Cooper, A., Kummerfeld, J. K., Dauchot, O., Biroli, G., Harrowell, P., and Reichman, D. R. (2009c). Avalanches and dynamical correlations in supercooled liquids. arXiv.org:0912.0193.
- Cates, M. E., Wittmer, J. P., Bouchaud, J. P., and Claudin, P. (1998). *Phys. Rev. Lett.*, **81**(9), 1841.
- Cipelletti, L. and Ramos, L. (2005). *J. Phys.-Cond. Matt.*, **17**(6), R253–R285.
- Cohen-Addad, S. and Hohler, R. (2001). *Physical Review Letters*, **86**(20), 4700.
- Cortet, P. P., Bonamy, D., Daviaud, F., Dauchot, O., Dubrulle, B., and Renouf, M. (2009). Relevance of visco-plastic theory in a multi-directional inhomogeneous granular flow.
- da Cruz, F., Emam, S., Prochnow, M., Roux, J.N., and Chevoir, F. (2005). *Physical Review E*, **72**(2), 21309.
- Daerr, A. and Douady, S. (1999). *Nature*, **399**(6733), 241–243.
- Dauchot, O. (2007). In *Ageing and the Glass Transition* (ed. MPRS), Chapter 4, p. 161. Springer.
- Dauchot, O., Marty, G., and Biroli, G. (2005). *Phys. Rev. Lett.*, **95**(26), 265701.
- Deboeuf, S., Bertin, EM, Lajeunesse, E., and Dauchot, O. (2003). *The European Physical Journal B-Condensed Matter and Complex Systems*, **36**(1), 105–113.
- Deboeuf, S., Dauchot, O., Staron, L., Mangeney, A., and Vilotte, J.P. (2005). *Physical Review E*, **72**(5), 51305.

- Deboeuf, S., Lajeunesse, E., Dauchot, O., and Andreotti, B. (2006). *Physical review letters*, **97**(15), 158303.
- Djaoui, L. and Crassous, J. (2005). *Granular Matter*, **7**(4), 185–190.
- Dollet, B., Elias, F., Quilliet, C., Raufaste, C., Aubouy, M., and Graner, F. (2005). *Physical Review E*, **71**(3), 31403.
- du Pont, S. C., Fischer, R., Gondret, P., Perrin, B., and Rabaud, M. (2005). *Phys. Rev. Lett.*, **94**, 048003.
- Duran, J. (2000). *Sands, powders, and grains: An introduction to the physics of granular materials*. Springer, NY.
- Duri, A., Sessoms, D. A., Trappe, V., and Cipelletti, L. (2009). *Physical Review Letters*, **102**(8), 085702–4. DOI: 10.1103/PhysRevLett.102.085702.
- Durian, D. J. (1995). *Physical Review Letters*, **75**(26), 4780–4783.
- Durian, D. J. (1997). *Physical Review E*, **55**(2), 1739–1751.
- Durian, D. J., Weitz, D. A., and Pine, D. J. (1991). *Science*, **252**(5006), 686–688.
- E. Janiaud, D. Weaire and Hutzler, S. (2006). *Phys. Rev. Lett.*, **97**, 038302.
- Earnshaw, J. C. and Jaafar, A. H. (1994). *Physical Review E*, **49**, 5408.
- Ediger, M. D. (2000). *Annu. Rev. Phys. Chem.*, **51**, 99–128.
- Ellenbroek, W. G., Zeravcic, Z., van Saarloos, W., and van Hecke, M. (2009). *Europhysics Letters*, **87**(3), 34004.
- Ertas, D. and Halsey, T.C. (2002). *Europhys. Lett.*, **60**, 931.
- Fenistein, D., van de Meent, J. W., and van Hecke, M. (2004). *Physical Review Letters*, **92**(9), 094301.
- G. Debregeas, H. Tabuteau and di Meglio, J.M. (2001). *Phys. Rev. Lett.*, **87**, 178305.
- G. Katgert, M. E. Mobius and van Hecke, M. (2008). *Phys. Rev. Lett.*, **101**, 058301.
- Garrahan, Juan P. and Chandler, David (2002). *PRL*, **89**, 035704.
- Geng, Junfei and Behringer, R. P. (2005, Jan). *Phys. Rev. E*, **71**(1), 011302.
- Gittings, A. S. and Durian, D. J. (2006). *Appl. Opt.*, **45**, 2199–2204.
- Gittings, A. S. and Durian, D. J. (2008). *Physical Review E*, **78**(6), 066313.
- Glotzer, S. C. (2000). *J. Non-Cryst. Solids*, **274**(1-3), 342–355.
- Goldhirsch, I (2003). *Annual Review Of Fluid Mechanics*, **35**, 267.
- Gopal, A. D. and Durian, D. J. (1995). *Physical Review Letters*, **75**(13), 2610–2613.
- Gopal, A. D. and Durian, D. J. (1997). *J. Opt. Soc. Am. A*, **14**(1), 150–155.
- Gopal, A. D. and Durian, D. J. (1999). *Journal of Colloid and Interface Science*, **213**(1), 169–178.
- Gopal, A. D. and Durian, D. J. (2003). *Physical Review Letters*, **91**(18), 188303.
- Habdas, P., Schaar, D., Levitt, A.C., and Weeks, E.R. (2004). *Europhysics Letters*, **67**(3), 477–483.
- Hatano, T. (2008). *arXiv:0804.0477v2*.
- Herdttle, T. and Aref, H. (1992). *Journal of Fluid Mechanics*, **241**, 233–60.
- Howell, D., Behringer, R.P., and Veje, C. (1999). *Phys. Rev. Lett.*, **82**(26), 5241–5244.
- I. K. Ono, S. Tewari, S.A. Langer and Liu, A. J. (2003). *Phys. Rev. E*, **67**, 061503.
- Iordanoff, I. and Khonsari, MM (2004). *Journal of Tribology*, **126**, 137.
- Jaeger, H. M., Nagel, S. R., and Behringer, R. P. (1996). *Rev. Mod. Phys.*, **68**, 1259.
- Jop, P., Forterre, Y., and Pouliquen, O. (2005). *J. Fluid Mech.*, **541**, 167–192.
- Jop, P., Forterre, Y., and Pouliquen, O. (2006). *Nature*, **441**(7094), 727–730.

- Katsuragi, H., Abate, A. R., and Durian, D. J. (2009). *preprint submitted to themed issue of Soft Matter*.
- Keys, A. S., Abate, A. R., Glotzer, S. C., and Durian, D. J. (2007). *Nature Physics*, **3**(4), 260–264.
- Khakhar, D. V., Orpe, A. V., Andresén, P., and Ottino, J. M. (2001). *J. Fluid Mech.*, **441**, 255.
- Komatsu, T. S., Inagaki, S., Nakagawa, N., and Nasuno, S. (2001). *Phys. Rev. Lett.*, **86**, 1757.
- Kraynik, A.M. (1988). *Ann. Rev. Fluid Mech.*, **20**, 325–357.
- Lacevic, N., Starr, F. W., Schroder, T. B., and Glotzer, S. C. (2003). *J. Chem. Phys.*, **119**(14), 7372–7387.
- Lauridsen, J., Chanan, G., and Dennin, M. (2004). *Physical Review Letters*, **93**(1), 018303.
- Lechenault, F., Candelier, R., Dauchot, O., Bouchaud, J. P., and Biroli, G. (2010). Super-diffusion around the rigidity transition: Levy and the lilliputians. [arXiv.org:1001.1765](https://arxiv.org/abs/1001.1765).
- Lechenault, F., Dauchot, O., Biroli, G., and Bouchaud, JP (2008a). *Europhysics Letters*, **83**, 46003.
- Lechenault, F., Dauchot, O., Biroli, G., and Bouchaud, J.-P. (2008b). *Europhysics Letters*, **83**.
- Lemaître, A. (2002). *Physical Review Letters*, **89**(19), 195503.
- Lemieux, P.-A. and Durian, D. J. (2000). *Phys. Rev. Lett.*, **85**, 4273.
- Liu, A. J. and Nagel, S. R. (ed.) (2001). *Jamming and Rheology: Constrained Dynamics on Microscopic and Macroscopic Scales*. Taylor and Francis, NY.
- Liu, A. J., Ramaswamy, S., Mason, T. G., Gang, H., and Weitz, D. A. (1996). *Physical Review Letters*, **76**(16), 3017–20.
- Losert, W., Bocquet, L., Lubensky, TC, and Gollub, JP (2000). *Physical Review Letters*, **85**(7), 1428–1431.
- Marty, G. and Dauchot, O. (2005). *Phys. Rev. Lett.*, **94**(1), 15701.
- Mayer, P., Bissig, H., Berthier, L., Cipelletti, L., Garrahan, J. P., Sollich, P., and Trappe, V. (2004). *Physical Review Letters*, **93**(11), 115701.
- M.E. Mobius, G. Katgert and van Hecke, M. (2008). [arXiv:cond-mat/0811-0534](https://arxiv.org/abs/cond-mat/0811-0534).
- MiDi, GDR (2004). *The European Physical Journal E: Soft Matter and Biological Physics*, **14**(4), 341–365.
- Mills, P., Loggia, D., and Texier, M. (1999). *Europhys. Lett.*, **45**, 733.
- Mueth, D. M., Debregeas, G. F., Karczmart, G. S., Eng, P. J., Nagel, S. R., and Jaeger, H. M. (2000). *Nature*, **406**(6794), 385–9.
- Nedderman, R.M. (1992). *Statics and Kinematics of Granular Materials*. Cambridge University Press, Cambridge.
- O’Hern, C.S., Silbert, L.E., Liu, A.J., and Nagel, S.R. (2003a). *Phys. Rev. E*, **68**(1), 11306.
- O’Hern, C. S., Silbert, L. E., Liu, A. J., and Nagel, S. R. (2003b). *Phys. Rev. E*, **68**(1), 011306.
- Okuzono, T. and Kawasaki, K. (1995). *Physical Review E*, **51**(2), 1246–53.
- Olsson, P. and Teitel, S. (2007). *Phys. Rev. Lett.*, **99**, 178001.

xxx *References*

- Pouliquen, Olivier, Belzons, M, and Nicolas, M (2003). *Ph. Rev. Lett.*, **91**, 014301.
- Prud'homme, Robert K. and Khan, Saad A. (1996). *Foams: Theory, Measurements, and Applications*. Marcel Dekker Inc., New York.
- Rajchenbach, J. (1990). *Phys. Rev. Lett.*, **65**, 2221.
- Richard, P., Valance, A., Metayer, J. F., Sanchez, P., Crassous, J., Louge, M., and Delannay, R. (2008). *Phys. Rev. Lett.*, **101**(24), 248002.
- Ritort, F. and Sollich, P. (2003). *Advances in Physics*, **52**(4), 219–342.
- Saint-Jalmes, A. and Durian, D. J. (1999). *Journal of Rheology*, **43**(6), 1411–1422.
- Savage, S.B. (1998). *Journal of Fluid Mechanics*, **377**, 1–26.
- Savage, S.B. and Jeffrey, D.J (1981). *J. Fluid Mech.*, **110**, 255.
- Sessoms, David A., Bissig, Hugo, Duri, Agnes, Cipelletti, Luca, and Trappe, Veronique (2010). *Soft Matter*, **6**(13), 3030–3037. 1744-683X.
- Sillescu, H. (1999). *J. Non-Cryst. Solids*, **243**, 81–108.
- Toninelli, C., Biroli, G., and Fisher, D.S. (2006). *Phys. Rev. Lett.*, **96**(3), 35702.
- van Hecke, M. (2010). *J. Phys. Cond. Matt.*, **22**, 031101.
- Wang, Y. H., Krishan, K., and Dennin, M. (2006). *Physical Review E*, **74**(4), 041405.
- Weaire, D. and Hutzler, S. (1999). *The Physics of Foams*. Clarendon Press, New York.
- Wilson, A.J. (ed.) (1989). *Foams: Physics, Chemistry and Structure*. Springer-Verlag, New York.
- Wyart, M. (2005). *Ann. Phys. Fr*, **30**(3), 1–96.
- Y. H. Wang, K. Krishan, M. Dennin (2006). *Phys. Rev. E*, **73**, 031401.